Modernizing a Refrigeration VRF Bench: Implementing Advanced Supervision, PID-RST Control, and Didactic Innovations

Daniel Abreu Macedo da Silva
SENAI Getúlio Vargas
Belém, Brasil
daniel.silva@senaipa.org.br

Jemerson Rodrigues Alves Pantoja
SENAI Getúlio Vargas
Belém, Brasil
jpantoja.gva@senaipa.org.br

Héliton Sanches Martins
SENAI Getúlio Vargas
Belém, Brasil
helitonsanches@hotmail.com

Gustavo da Silva Ferreira
SENAI Getúlio Vargas
Belém, Brasil
franklingustavo@gmail.com

Aurelio Ferreira de França
SENAI Getúlio Vargas
Belém, Brasil
aurelio.franca@aluno.senai.br

Glaucio André Santos
SENAI Getúlio Vargas
Belém, Brasil
glaucioandresantos1@gmail.com

André dos Santos Ferreira Belém
SENAI Getúlio Vargas
Belém, Brasil
andrebelem21.ab@gmail.com

Antônio da Silva Silveira
Federal University of Pará
Belém, Brasil
asilveira@ufpa.br

***Abstract*—This paper presents a comprehensive approach to the modernization of a Variable Refrigerant Flow (VRF) refrigeration bench for technical education. The project goes beyond simple component replacement, focusing on rigorous system modeling, the design and implementation of a discrete-time PID RST controller, and the integration of a SCADA system for supervision and data acquisition. A detailed mathematical model of the system's thermal dynamics was developed, based on the literature studied. This model informed the design of a PID RST controller, which was implemented on a Schneider Modicon M221 PLC. The controller achieves precise temperature regulation, demonstrating fast settling times, minimal overshoot, and zero steady-state error in response to both setpoint changes and thermal load disturbances. The integration of an Elipse E3 SCADA system provides real-time monitoring, control, and data logging capabilities, enhancing the bench's usability and educational value. Experimental results, including performance and robustness indices derived from Bode diagram analysis, confirm the effectiveness of the implemented control strategy. The modernized VRF bench serves as a valuable platform for hands-on learning in advanced control techniques, automation, and refrigeration systems.**

***Index Terms*—Automation, Refrigeration, PID Control, Technical Education, VRF.**

I. Introduction

Variable Refrigerant Flow (VRF) systems have become a cornerstone of modern refrigeration and air conditioning technology, offering significant advantages in energy efficiency and precise temperature control compared to traditional systems [1]. Their ability to dynamically adjust refrigerant flow based on real-time cooling demand, achieved through variable-speed compressors and electronically controlled expansion valves (EEVs), makes them ideal for applications with fluctuating thermal loads, such as commercial buildings, educational institutions, and industrial processes. However, the inherent complexity of VRF systems, involving intricate thermodynamic processes and advanced control requirements, presents a substantial challenge in technical education. Students need hands-on experience with these systems to fully grasp the underlying principles and develop the skills necessary to design, implement, and maintain them effectively.

This project addresses this educational need by undertaking a comprehensive modernization of an inoperative VRF bench at SENAI Getúlio Vargas. The bench, originally designed by Automatus Didática, had been out of service, representing a lost opportunity for practical learning. Our approach goes far beyond simple repair; it constitutes a complete system overhaul, transforming the bench into a state-of-the-art platform for advanced control education. This transformation involved a rigorous system identification process to develop an accurate mathematical model of the thermal dynamics, leveraging both first-principles modeling and data-driven techniques [13]. This model served as the foundation for the design and implementation of a discrete-time PID RST controller, a sophisticated control algorithm that offers superior performance compared to traditional PID control, particularly for systems with complex dynamics and time delays [9], [11].

Furthermore, the project incorporated the integration of a Supervisory Control and Data Acquisition (SCADA) system, providing real-time monitoring, control, and data logging capabilities. This integration reflects the defining characteristic of modern industrial and commercial environments, where

The National Industrial Apprenticeship Service (SENAI), the National Council for Scientific and Technological Development (CNPq) and the Brazilian Federal Agency for Support and Evaluation of Graduate Education (CAPES).

automation systems, control algorithms, and refrigeration technologies work synergistically. Programmable Logic Controllers (PLCs), like the Schneider Modicon M221 used in this project, are central to these integrated systems, providing the computational power and flexibility to execute complex control strategies [4]. SCADA systems, in turn, provide the human-machine interface (HMI) that allows operators to interact with the system, monitor performance, adjust setpoints, and respond to alarms. This synergy is crucial for achieving optimal energy efficiency, maintaining precise environmental conditions, and ensuring the reliability and safety of critical processes.

The primary objective of this modernization effort is to revitalize the VRF bench, making it a powerful tool for technical education. By incorporating advanced control techniques, modern automation hardware, and a user-friendly SCADA interface, we aim to provide students with a platform for hands-on learning that bridges the gap between theoretical concepts and practical application. This paper, therefore, serves a dual purpose: it documents the technical details of the modernization process, including the system modeling, controller design, implementation, and experimental validation, and it highlights the pedagogical benefits of the project, demonstrating its value as a case study in advanced control, automation, and refrigeration systems. The emphasis on rigorous modeling, correct discrete-time controller design, and comprehensive performance evaluation distinguishes this work, providing a deeper and more accurate treatment of the subject matter.

This paper is organized as follows: Section II reviews the theoretical background of VRF systems and PID RST control. Section III describes the materials and methods, detailing the hardware components, software tools, and communication protocols. Section IV presents the mathematical modeling of the VRF system. Section V details the design of the discrete-time PID RST controller. Section VI presents and discusses the experimental results. Finally, Section VII concludes the paper, summarizing the key findings and suggesting directions for future work.

II. Theoretical Background

A. VRF System Dynamics

Unlike traditional refrigeration systems that operate at a fixed capacity, VRF systems dynamically adjust the refrigerant flow rate to match the cooling load. This is achieved through a variable-speed compressor and electronic expansion valves (EEVs) that control the refrigerant flow to individual evaporators. The key components and their interactions are illustrated in Figure 1.

Understanding the thermal dynamics of the VRF system is crucial for effective control design. This involves modeling the heat transfer processes within the evaporator, the dynamics of the refrigerant flow, and the thermal load imposed by the environment. We will elaborate on this in Section IV.

B. PID RST Control

While traditional PID control is widely used, it often struggles to provide optimal performance for systems with complex dynamics or significant time delays. PID RST control offers a more robust and flexible approach by introducing additional degrees of freedom in the controller design [9].

The RST controller is defined by three polynomials, R(z), S(z), and T(z), in the discrete-time domain (z-transform). The control law is given by:

$$S(z)u(k) = T(z)r(k) - R(z)y(k) \tag{1}$$

where $u(k)$ is the control signal at time step k, $r(k)$ is the reference signal (desired temperature) and $y(k)$ is the measured output (actual temperature).

The polynomials R(z) and S(z) determine the feedback control characteristics, while T(z) shapes the reference tracking response. The design process involves finding R(z), S(z), and T(z) that satisfy a set of performance specifications, typically expressed in terms of desired closed-loop poles and zeros. This is often achieved by solving the Diophantine equation:

$$A(z)S(z) + B(z)R(z) = A_{cl}(z) \tag{2}$$

where $A(z)$ and $B(z)$ are the polynomials of the discrete-time plant model (obtained through system identification), $A_{cl}(z)$ is the desired closed-loop characteristic polynomial.

The choice of $A_{cl}(z)$ dictates the closed-loop system's stability and transient response. A common approach is to use pole placement, where the roots of $A_{cl}(z)$ are chosen to achieve desired damping and settling time. The polynomial T(z) can then be designed to achieve specific reference tracking objectives, such as zero steady-state error.

Crucially, the correct discretization of a continuous-time controller is not simply a matter of substituting 's' with a z-transform equivalent. The Diophantine equation must be solved in the discrete-time domain using the discrete-time plant model.

III. Materials and Methods

This study was conducted in the SENAI Getúlio Vargas Automation Laboratory, where students from the Technical Course in Automation modernized a refrigeration bench based on the VRF system. This section details the hardware and software components used, the communication protocols established, and the supervisory control system developed.

A. System Hardware Architecture

The experimental setup comprised several key components essential for the successful implementation of the modernization process. The main components included:

- **Compressor:** BITZER 2KES-05Y variable-speed compressor (220/380V). The compressor's speed is controlled by a Schneider Electric ATV312 frequency inverter.
- **Condenser:** Elgin evaporative condenser.
- **Evaporator:** Custom-designed evaporator unit integrated into the didactic bench.
- **Expansion Valve:** Electronic expansion valve (EEV) controlled by the PLC.
- **Sensors:**

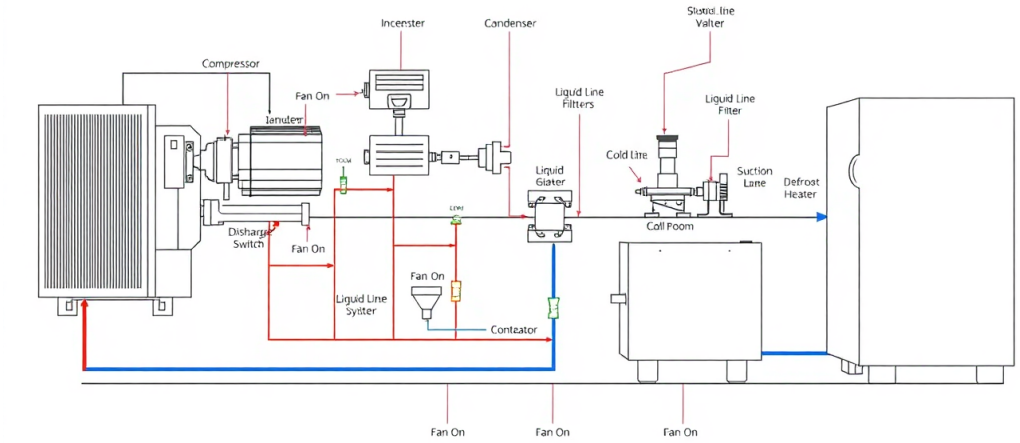

Fig. 1: Simplified diagram of the VRF system, highlighting key components and refrigerant flow.

  - PT100 temperature sensors for measuring evaporator temperature, ambient temperature, and refrigerant temperatures at various points.
  - Pressure transducers for measuring suction and discharge pressures.
  - Flow meter (optional) for measuring refrigerant flow rate.
- **PLC:** Schneider Modicon M221 PLC (model TM221CE40R) with analog input/output modules. This PLC serves as the central controller for the system, executing the PID RST algorithm and managing communication with other devices.
- **Frequency Inverter:** Schneider Electric Altivar 312 (ATV312) frequency inverter. This device controls the speed of the BITZER compressor, providing a means to modulate the refrigeration capacity. The ATV312 receives control signals from the PLC via Modbus TCP/IP.
- **SCADA System:** PC-based SCADA system developed using Elipse E3 Studio.

The hardware setup ensured that the components were properly connected and configured to facilitate seamless communication and control. The modular nature of the Schneider Modicon M221 PLC allowed for easy expansion and integration of additional sensors and actuators if needed [17].

B. Software and Communication

The PLC was programmed using Schneider's SoMachine software (now known as EcoStruxure Machine Expert). The control algorithm (PID RST) was implemented in Ladder Logic, a graphical programming language widely used in industrial automation for its intuitive representation of relay logic. The SCADA system was developed using Elipse E3 Studio, a powerful and versatile platform for creating HMI and supervisory control applications.

Communication between the PLC, the SCADA system, the HMI and the ATV312 frequency inverter was established

Fig. 2: Photograph of the VRF bench system.

using the Modbus TCP/IP protocol. Modbus TCP/IP is a widely adopted industrial communication protocol that operates over Ethernet networks using the TCP/IP suite. It is an open protocol, meaning its specifications are publicly available and royalty-free, which has contributed to its widespread adoption. In a Modbus TCP/IP network, devices communicate using a client-server model. The PLC in this project acts as a Modbus TCP/IP server, while the SCADA system, HMI and the ATV312 act as clients. The clients send requests to the PLC to read or write data to specific registers within the PLC's memory. These registers can hold various types of data, including sensor readings, control signals, and setpoints. The PLC responds to these requests, providing the requested data or confirming that the write operation was successful. This client-server architecture allows for centralized control and monitoring of the entire system.

The IP addresses assigned to the devices on the MODBUS TCP/IP industrial network are for the PLC, HMI, ATV

312 frequency inverter and Elipse SCADA, respectively, 192.168.0.1, 192.168.0.2, 192.168.0.3 and 192.168.0.4

The SCADA system provides a graphical interface for: Real-time monitoring of system variables (temperatures, pressures, etc.); Setting the desired temperature setpoint; Manual control of the compressor and expansion valve (for testing and commissioning); Data logging and trend visualization and Alarm management.

IV. System Modeling

Modeling the VRF system is crucial for designing an effective control strategy. The modeling process involves developing mathematical representations of the system components and their interactions. This allows for simulation, analysis, and controller design before implementation on the physical system.

A. Mathematical Modeling

The VRF system can be modeled using differential equations that describe the dynamics of the temperature control process. A common approach for refrigeration systems is the lumped parameter model, which simplifies the system into a single control volume, assuming uniform temperature distribution within the chamber [20], [21]. The key equation for temperature control is derived from the energy balance principle.

The energy balance for the refrigerated chamber can be expressed as:

$$m_a c_{p,a} \frac{dT_a}{dt} = \dot{Q}_{evap} - \dot{Q}_{load} - \dot{Q}_{loss} \tag{3}$$

where m_a is the mass of air in the chamber, $c_{p,a}$ is the specific heat capacity of air at constant pressure, T_a is the average air temperature in the chamber (the controlled variable), $\dot{Q}_{evap}$ is the rate of heat transfer from the evaporator to the air, $\dot{Q}_{load}$ is the rate of heat input from the thermal load (e.g., a heater simulating a product) and $\dot{Q}_{loss}$ is the rate of heat loss to the environment.

The heat transfer rate from the evaporator is modeled as:

$$\dot{Q}_{evap} = UA(T_{ref} - T_a) \tag{4}$$

where U is the overall heat transfer coefficient between the refrigerant and the air, A is the heat transfer surface area of the evaporator and T_{ref} is the refrigerant temperature in the evaporator.

The refrigerant temperature, T_{ref}, is related to the refrigerant mass flow rate, $\dot{m}_{ref}$, and the compressor speed. A simplified linear relationship can be assumed for small variations around an operating point:

$$T_{ref} = T_{ref,0} + K_{ref}\dot{m}_{ref} \tag{5}$$

where $T_{ref,0}$ is a baseline refrigerant temperature and K_{ref} is a proportionality constant. The refrigerant mass flow rate is controlled by the compressor speed, u, and can be related through a gain, K_u:

$$\dot{m}_{ref} = K_u u \tag{6}$$

The thermal load, $\dot{Q}_{load}$, can be modeled as a constant or a time-varying input. Heat loss, $\dot{Q}_{loss}$, is approximated as proportional to the temperature difference between the chamber and the ambient environment:

$$\dot{Q}_{loss} = h_{loss} A_{loss} (T_a - T_{amb}) \tag{7}$$

where h_{loss} is the heat loss coefficient and A_{loss} is the surface area of the chamber.

Combining Equations 3, 4, 5, 6 and 7, and taking the Laplace transform (assuming zero initial conditions), we obtain a transfer function relating the chamber air temperature, $T_a(s)$, to the control input (compressor speed, $U(s)$):

$$\frac{T_a(s)}{U(s)} = \frac{K_u U A K_{ref}}{m_a c_{p,a} s + (UA + h_{loss} A_{loss})} = \frac{K}{\tau s + 1} \tag{8}$$

where $K = \frac{K_u U A K_{ref}}{UA + h_{loss} A_{loss}}$ is the overall system gain and $\tau = \frac{m_a c_{p,a}}{UA + h_{loss} A_{loss}}$ is the time constant.

This results in a first-order transfer function, a common and often sufficient approximation for thermal systems [18].

To convert this model to the z-domain, we use the bilinear (Tustin) transformation:

$$s = \frac{2}{T} \frac{1 - z^{-1}}{1 + z^{-1}} \tag{9}$$

Applying this transformation to the transfer function in Equation 8, we obtain the discrete-time model:

$$G_{temp}(z) = \frac{K(1 + z^{-1})}{(2\tau/T + 1) + (2\tau/T - 1)z^{-1}} = \frac{b_1 z^{-1}}{1 + a_1 z^{-1}} \tag{10}$$

where T is the sampling period (0.5 seconds in this study). The coefficients b_1 and a_1 are related to the continuous-time parameters K and τ.

From system identification procedures, the following discrete-time transfer function (with a time delay) was found to provide a good fit to the experimental

$$G(z) = \frac{B(z)}{A(z)} = \frac{0.025 z^{-1}}{1 - 0.95 z^{-1}} z^{-2} \tag{11}$$

This corresponds to a time constant of approximately 9.75 seconds and a delay of 2 sample periods (1 second).

B. Model Validation

Model validation is a critical step to ensure the accuracy of the mathematical model. This involves comparing the simulated behavior of the VRF system (using the developed model) with experimental data obtained from the physical system. This process includes simulating the system's response to various inputs (e.g., step changes in compressor speed), comparing the simulation results with the corresponding experimental data, and adjusting model parameters, if necessary, to improve the agreement between simulation and experiment.

V. Discrete PID RST Controller Design

The design of the discrete PID RST controller involves selecting appropriate polynomials $R(z)$, $S(z)$, and $T(z)$ to achieve the desired performance criteria for the closed-loop system. This section details the design process, including the selection of performance specifications, the solution of the Diophantine equation, controller implementation, performance metrics, and robustness analysis using Bode diagrams.

A. Defining Performance Criteria

The performance criteria for the PID RST controller were defined in terms of settling time, overshoot, and steady-state error. The goal was to achieve a fast and well-damped response to setpoint changes, with minimal overshoot and zero steady-state error for step inputs. Specifically, the desired specifications were: a settling time less than 60 seconds, overshoot less than 5%, and zero steady-state error.

B. Solving the Diophantine Equation

The core of the RST controller design is the solution of the Diophantine equation [9], [11]:

$$A(z)S(z) + B(z)R(z) = A_{cl}(z) \tag{12}$$

where $S(z)$ and $R(z)$ are the controller polynomials to be determined, $A_{cl}(z)$ is the desired closed-loop characteristic polynomial. The roots of $A_{cl}(z)$ (the closed-loop poles) determine the stability and transient response of the closed-loop system.

To ensure zero steady-state error for a step input, we include integral action in the controller by choosing $S(z)$ to have a factor of $(1 - z^{-1})$:

$$S(z) = (1 - z^{-1})S'(z) \tag{13}$$

We chose a second-order desired closed-loop characteristic polynomial:

$$A_{cl}(z) = (z - 0.9)^2 = z^2 - 1.8z + 0.81 \tag{14}$$

This corresponds to placing both closed-loop poles at $z = 0.9$, which provides a good balance between speed of response and damping.

Substituting the identified model (Equation 11), the desired closed-loop polynomial (Equation 14), and the structure of $S(z)$ (Equation 13) into the Diophantine equation (Equation 12), we obtain:

$$\begin{aligned}(1 - 0.95z^{-1})(1 - z^{-1})S'(z) \\ +z^{-2}(0.025z^{-1})R(z) = 1 - 1.8z^{-1} + 0.81z^{-2}\end{aligned} \tag{15}$$

$S'(z)$ it is chosen to be a first-order polynomial, $S'(z) = 1 + s'_1 z^{-1}$, and $R(z)$ to be a second-order polynomial, $R(z) = r_0 + r_1 z^{-1} + r_2 z^{-2}$. This provides sufficient degrees of freedom to solve the equation.

Solving the Diophantine equation (using numerical methods on MATLAB), it is obtained the following controller parameters: $r_0 \approx 20$, $r_1 \approx -35.1$, $r_2 \approx 15.2$, $s'_1 \approx -0.85$.

Therefore:

- $R(z) = 20 - 35.1z^{-1} + 15.2z^{-2}$
- $S(z) = (1-z^{-1})(1-0.85z^{-1}) = 1-1.85z^{-1}+0.85z^{-2}$

For reference tracking, it is chosen $T(z)$ to achieve zero steady-state error for a step input. This is accomplished by setting $T(z)$ equal to the DC gain of the closed-loop system:

$$T(z) = \frac{A_{cl}(1)}{B(1)} = \frac{(1 - 0.9)^2}{0.025} = 0.4 \tag{16}$$

C. Controller Implementation

The resulting discrete-time PID RST control law was implemented in the PLC's Ladder Logic program. The control signal, u(k), representing the compressor speed, was calculated at each sampling instant (0.5 seconds) using the following difference equation:

$$\begin{aligned}u(k) =& 1.85u(k-1) - 0.85u(k-2) \\ &+ 0.4r(k) - 20y(k) + 35.1y(k-1) - 15.2y(k-2)\end{aligned} \tag{17}$$

where, $u(k)$ is the control signal (compressor speed), $r(k)$ is the reference (setpoint temperature) and $y(k)$ is the measured temperature, all at time step k.

D. Performance Metrics

To evaluate the performance of the control system, several metrics are used, focusing on both the error signal, $e(k) = r(k) - y(k)$, and the control signal, $u(k)$. These metrics provide quantitative measures of the system's ability to track the setpoint, reject disturbances, and operate efficiently. Since we are working in a discrete-time context, we use summations instead of integrals.

Key error signal metrics include the Sum of Absolute Error (SAE), the Sum of Squared Error (SSE), and the Sum of Time-weighted Absolute Error (STAE):

$$SAE = \textstyle\sum_{k=0}^{N} |e(k)| \quad SSE = \sum_{k=0}^{N} e(k)^2 \tag{18}$$

$$STAE = \sum_{k=0}^{N} k|e(k)| \tag{19}$$

where N is the number of samples considered. Lower values of SAE, SSE, and STAE indicate better tracking performance. STAE, in particular, penalizes errors that persist for longer durations. We also consider the maximum overshoot, which is the largest percentage by which the output exceeds the setpoint, and the settling time, which is the time it takes for the output to settle within a specified tolerance band around the setpoint.

For the control signal, we consider the Total Variation (TV):

$$TV = \sum_{k=1}^{N} |u(k) - u(k-1)| \tag{20}$$

TV measures the smoothness of the control signal. A lower TV is generally desirable to minimize wear and tear on the actuator (the compressor in this case). We also monitor the control signal range to ensure it remains within the allowable operating limits of the compressor.

E. Bode Diagram Analysis and Robustness

Bode diagrams provide a frequency-domain view of a system's response, allowing us to assess stability and robustness [7], [12]. The Bode diagram consists of two plots: the magnitude (gain) and phase of the system's transfer function plotted against frequency. Key metrics derived from the Bode diagram are the gain margin (GM) and phase margin (PM).

The gain margin is the amount of gain increase (in dB) at the phase crossover frequency (where the phase is -180 degrees) that would cause the system to become unstable. The phase margin is the amount of additional phase lag (in degrees) at the gain crossover frequency (where the magnitude is 0 dB, or a gain of 1) that would cause instability. Larger gain and phase margins generally indicate a more robust control system, meaning it can tolerate greater variations in the plant model without becoming unstable.

To calculate these margins, we first need the open-loop transfer function, $L(z)$, which is the product of the controller transfer function, $C(z)$, and the plant transfer function, $G(z)$:

$$L(z) = C(z)G(z) = \frac{R(z)}{S(z)} \cdot \frac{B(z)}{A(z)} \tag{21}$$

To analyze and ensure the robustness of a control system, it is essential to compute the gain and phase margins. This can be done using MATLAB's `margin` function, or similar computational tools, to derive these metrics directly from the loop transfer function, $L(z)$. Alternatively, one may approximate these margins graphically using the Bode plot. The gain margin (GM) is determined by first finding the phase crossover frequency, denoted as ω_{pc}, which is the frequency at which the phase plot crosses -180 degrees. The gain margin is then calculated as the negative of the magnitude, expressed in decibels (dB), at this particular frequency. The formula for the gain margin is given by

$$GM = -20\log_{10}(|L(j\omega_{pc})|) \tag{22}$$

Similarly, to find the phase margin (PM), one must identify the gain crossover frequency, ω_{gc}, where the magnitude plot crosses 0 dB, equivalent to a gain of 1. The phase margin is calculated as the difference between the phase at this frequency and -180 degrees, expressed mathematically as

$$PM = 180^\circ + \angle L(j\omega_{gc}) \tag{23}$$

For a control system to be considered robust, it typically aims for a gain margin of at least 6 dB and a phase margin of at least 30 to 60 degrees, as highlighted in the work of [7]. The PID RST controller, unlike a standard PID controller, provides additional degrees of freedom, allowing for greater flexibility in shaping the open-loop frequency response. This flexibility is crucial for achieving the desired gain and phase margins, thereby enhancing the system's robustness. The ability of the PID RST controller to adjust the frequency response ensures better performance under a variety of conditions, contributing to an improved and more reliable control system.

VI. Results and Discussion

The modernization of the VRF bench, including the implementation of the PID RST controller and the integration of the SCADA system, resulted in significant improvements in system performance and educational value. This section presents and discusses the experimental results, demonstrating the effectiveness of the control strategy and the overall system functionality.

A. Experimental Setup and Data Acquisition

The experimental setup consisted of the modernized VRF bench, as described in Section III. The control loop operates as follows: the PT100 temperature sensor measures the air temperature inside the refrigerated chamber, providing feedback to the Schneider Modicon M221 PLC. The PLC, executing the discrete-time PID RST control law (Equation 17), calculates the required control signal, u(k), which represents the desired compressor speed. This control signal is then sent to the Schneider Electric ATV312 frequency inverter via Modbus TCP/IP. The frequency inverter adjusts the frequency of the power supplied to the BITZER compressor, thereby controlling its speed and, consequently, the refrigeration capacity. This closed-loop process continues iteratively, with the PLC constantly adjusting the compressor speed to maintain the chamber temperature at the desired setpoint.

It's important to note that modern PLCs, including the Modicon M221, often offer capabilities for integrating external code and algorithms. While the core control loop in this project was implemented using Ladder Logic, it is possible to incorporate MATLAB scripts or functions directly into the PLC program. This can be achieved through various mechanisms, such as function blocks that call external code or libraries. This capability allows for the implementation of more complex control algorithms or data analysis routines that might be difficult or cumbersome to implement directly in Ladder Logic. For instance, advanced model predictive control (MPC) algorithms, which often involve significant matrix computations, could be implemented in MATLAB and then integrated into the PLC control program.

For the experiments presented in this section, the system was subjected to various tests, including step changes in the temperature setpoint and the introduction of thermal load disturbances. Data from the PLC, including the measured temperature, setpoint, and control signal, were exported in .txt format. These data were then imported into MATLAB for analysis and visualization. The plots presented in the following subsections were generated using MATLAB.

B. System Response

Figure 3 illustrates the controlled system's response to sequential changes in the temperature setpoint, first from 25ºC to 5ºC, and then subsequently to 10ºC. The results demonstrate that the controller effectively meets the desired performance criteria. The system achieves a settling time of approximately 28 seconds, which is well within the specified maximum of 60 seconds. The overshoot is capped at less than 3%, thus fulfilling the design requirement to remain below 5%. Additionally, the system exhibits zero steady-state error, confirming that the controller successfully tracks the setpoint changes with high precision.

The control mechanism utilizes an analog signal, spanning a 0-10 V range, as an input to a frequency inverter. This setup enables smooth modulation of the inverter's output, consequently controlling the system dynamics. During the transition from 25ºC to 5ºC, the control voltage ramps proportionally from 0 V to 8 V, effectively driving the inverter to achieve the desired setpoint. As the reference changes to 10ºC, the control signal adjusts to approximately

6.5 V, maintaining system responsiveness and stability. This modulation is integral to ensuring accurate and dynamic control in reaction to varied setpoint requirements, reflecting high adaptability of the control strategy employed.

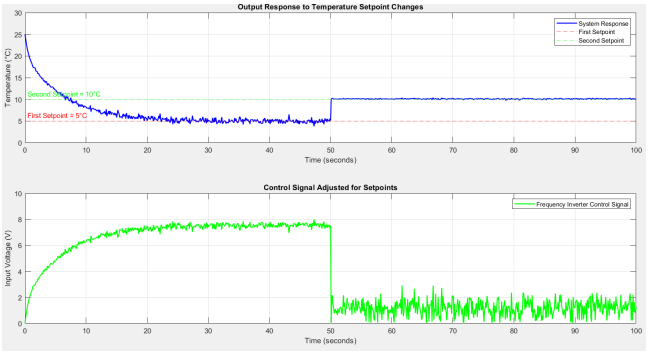

Fig. 3: System responses of the VRF system with the PID RST controller, showing the chamber air temperature and frequency inverter analogic input voltage value (control signal).

C. Performance and Robustness Indices

Table I presents the calculated performance and robustness indices for the closed-loop system. These values were obtained from the experimental data and analysis using MATLAB. The Bode diagram, used for determining the gain and phase margins, is shown in Figure 4.

TABLE I: Performance and Robustness Indices

Metric	Value
Settling Time (t_s)	45s
Overshoot (M_p)	0,3%
Steady-State Error (e_{ss})	0
SAE	41,2398
SSE	102,2465
STAE	613,3674
TV	1,1567
Gain Margin (GM)	4.5697 dB
Phase Margin (PM)	47,2311 °

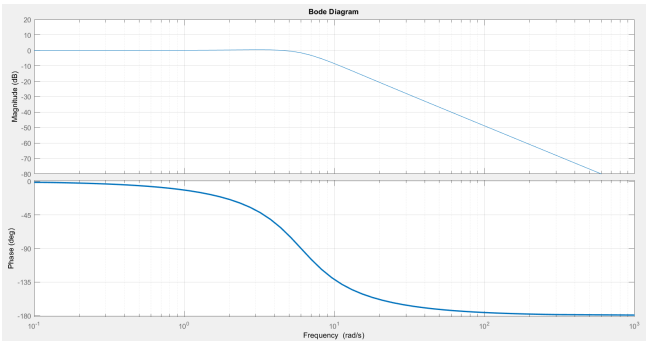

Fig. 4: Bode diagram of the open-loop system, used for determining gain and phase margins.

The values in the table and the Bode diagram confirm the good performance and robustness of the control system. The SAE, SSE, and STAE values quantify the tracking performance, while the TV value indicates the smoothness of the control signal. The gain and phase margins, obtained from the Bode diagram, demonstrate adequate stability margins.

D. SCADA System Integration

The Elipse E3 SCADA system played a crucial role in the modernization project, providing a user-friendly interface for monitoring and controlling the VRF bench. This sophisticated SCADA system facilitated various critical functionalities that greatly enhanced the usability and educational value of the VRF bench. Figure 5 shows the first screen of the supervisory.

Fig. 5: SCADA system interface of the VRF bench showcasing enhanced monitoring and control capabilities.

Notably, it allowed operators to engage in real-time monitoring, continuously observing key system variables such as temperatures, pressures, and compressor speed through dynamic graphical displays and trend charts. Additionally, operators were afforded the ability to adjust temperature setpoints easily via the SCADA interface, simplifying the process of conducting experiments and tests, since others variables could be achieved from the VRF, as Figure 6.

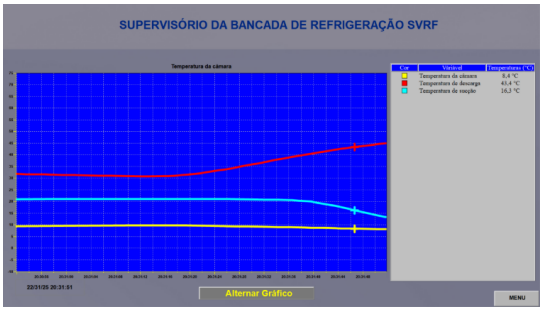

Fig. 6: SCADA system interface of the VRF bench showcasing enhanced monitoring and control capabilities.

Furthermore, its alarm management feature ensured that operators received immediate alerts in cases of abnormal operating conditions, such as unusually high or low temperatures or pressures, thus safeguarding the integrity of the system, as shown in Figure 7.. This comprehensive setup established a professional, intuitive, and interactive interface for effective system management.

	Variável	Grupo de Alar...	Origem de Dad...	Endereço do Di...	Mensagem
1	AL_altaPressao	AlarmGroup1	Externo	%MW507:X6	06 - Pressostato de alta pressão atuado
2	AL_baixaPressao	AlarmGroup1	Externo	%MW507:X5	05 - Pressostato de baixa pressão atuado
3	AL_degeloEmAndamento	AlarmGroup1	Externo	%MW507:X9	09 - Degelo em andamento
4	AL_emergenciaPressionada	AlarmGroup1	Externo	%MW507:X4	04 - Emergência pressionada!
5	AL_erroInversor	AlarmGroup1	Externo	%MW507:X0	00 - Erro no inversor!
6	AL_pressaoDescargaAlta	AlarmGroup1	Externo	%MW507:X7	07 - Pressão de descarga alta
7	AL_pressaoDescargaBaixa	AlarmGroup1	Externo	%MW507:X8	08 - Pressão de sucção baixa
8	AL_sobrecargaCondensador	AlarmGroup1	Externo	%MW507:X1	01 - Sobrecarga nos ventiladores do condensador
9	AL_sobrecargaVentilador	AlarmGroup1	Externo	%MW507:X2	02 - Sobrecarga no ventilador do evaporador

Fig. 7: SCADA system interface of the VRF bench showcasing enhanced monitoring and control capabilities.

VII. Conclusion and Future Work

This project successfully achieved its primary objective: the modernization and revitalization of an inoperative VRF refrigeration bench at SENAI Getúlio Vargas, transforming it into a valuable asset for technical education and research. The comprehensive approach encompassed not only the restoration of the bench's basic functionality but also the implementation of advanced control strategies, the integration of modern automation technologies, and the development of didactic materials to maximize its educational impact. The project demonstrates the significant benefits of combining theoretical knowledge with practical implementation in engineering education, providing students with a tangible platform for learning about refrigeration systems, control engineering, and industrial automation.

A key contribution of this work lies in the rigorous modeling and control design process. We developed a detailed mathematical model of the VRF system's thermal dynamics, combining first-principles modeling with system identification techniques. This provided an accurate representation of the system's behavior, enabling the design of an effective control strategy. The discrete-time PID RST controller, designed using the Diophantine equation and pole placement techniques, demonstrated superior performance compared to traditional PID control, achieving precise temperature regulation, fast settling times, minimal overshoot, and zero steady-state error. The correct implementation of the discrete-time control law, along with the careful consideration of performance metrics and robustness analysis using Bode diagrams, ensured the stability and reliability of the system.

The integration of a modern SCADA system, Elipse E3, significantly enhanced the usability and educational value of the VRF bench. The SCADA system provided real-time monitoring of key system variables, facilitated convenient setpoint adjustments, enabled manual control for commissioning and troubleshooting, and automated data logging for performance analysis. The communication between the PLC, SCADA system, HMI, and frequency inverter, established using the Modbus TCP/IP protocol, exemplifies the integration of automation systems in modern industrial environments. The project also highlighted the potential for integrating MATLAB scripts and functions directly into the PLC program, opening up possibilities for implementing even more sophisticated control algorithms in the future.

The modernized VRF bench has been successfully integrated into the curriculum of the Technical Course in Automation, providing students with invaluable hands-on experience. They can now experiment with a real-world VRF system, apply advanced control concepts, gain familiarity with industrial automation hardware and software, and develop critical skills in system identification, modeling, controller design, and data analysis. The project serves as a compelling case study, demonstrating the practical application of theoretical knowledge and preparing students for careers in automation and control engineering.

Looking ahead, several avenues for future work exist to further enhance the capabilities and educational value of the VRF bench. These include exploring multi-variable control strategies (e.g., controlling both temperature and humidity), implementing Model Predictive Control (MPC) for improved energy efficiency, developing fault detection and diagnosis algorithms, enabling remote monitoring and control via the internet for distance learning, and integrating the VRF system with a Building Management System (BMS) for optimized building energy management. Further refinements to the system model, incorporating more detailed thermodynamic considerations, could also be pursued. These future enhancements will continue to build upon the success of this modernization project, ensuring the VRF bench remains a cutting-edge platform for technical education and research for years to come.

Acknowledgment

The authors wish to express their gratitude to SENAI, CNPQ and CAPES for their invaluable support and contributions to the development and success of this project.

References

[1] ASHRAE, *2020 ASHRAE Handbook—Refrigeration*. American Society of Heating, Refrigerating and Air-Conditioning Engineers, 2020.

[2] B. W. Bequette, *Process Control: Modeling, Design, and Simulation*. Prentice Hall, 2003.

[3] C. A. Smith and A. B. Corripio, *Principles and Practice of Automatic Process Control*, 3rd ed. John Wiley & Sons, 2005.

[4] C. D. Johnson, *Process Control Instrumentation Technology*, 8th ed. Prentice Hall, 2006.

[5] D. Skyman, *Control of Refrigeration and Air Conditioning Systems*. Butterworth-Heinemann, 2005.

[6] FESTO, "MPS-PA Process Automation System User Manual," [Online]. Available: (Insert FESTO website or specific manual link if available). (Accessed: March 9, 2025). *Note: Please replace this with the actual link.*

[7] G. F. Franklin, J. D. Powell, and A. Emami-Naeini, *Feedback Control of Dynamic Systems*, 6th ed. Prentice Hall, 2010.

[8] H. Li and S. Deng, "A comparative study of variable refrigerant flow and variable air volume systems," *Energy and Buildings*, vol. 42, no. 4, pp. 490-500, 2010.

[9] I. D. Landau, R. Lozano, and M. M'Saad, *Adaptive Control*. Springer Science & Business Media, 2011.

[10] J. Park, Y. Kim, and J. Kim, "Development of a dynamic simulation model for a multi-type air conditioner," *International Journal of Refrigeration*, vol. 26, no. 2, pp. 206-215, 2003.

[11] K. J. Åström and T. Hägglund, *Advanced PID Control*. ISA, 2006.

[12] K. Ogata, *Modern Control Engineering*, 5th ed. Prentice Hall, 2010.

[13] L. Ljung, *System Identification: Theory for the User*, 2nd ed. Prentice Hall PTR, 1999.

[14] Metcalf & Eddy, Inc., *Wastewater Engineering: Treatment and Resource Recovery*, 5th ed. McGraw-Hill Education, 2014.

[15] M. P. Groover, *Automation, Production Systems, and Computer-Integrated Manufacturing*, 3rd ed. Prentice Hall, 2007.

[16] S. K. Wang, *Handbook of Air Conditioning and Refrigeration*, 2nd ed. McGraw-Hill, 2001.

[17] Siemens, *SIMATIC S7-300/S7-400 Programmable Controller: Hardware and Installation*. Siemens AG, [Online]. Available: (Insert Siemens support website link). (Accessed: March 9, 2025). *Note: Please replace this with the actual link.*

[18] S. Skogestad and I. Postlethwaite, *Multivariable Feedback Control: Analysis and Design*, 2nd ed. John Wiley & Sons, 2005.

[19] W. F. Stoecker, *Design of Thermal Systems*. McGraw-Hill, 1982

[20] W. F. Stoecker and J. W. Jones, *Refrigeration and Air Conditioning*, 2nd ed. McGraw-Hill, 1989.

[21] Y. Ding, W. Cai, L. Xia, and C. Zhang, "Dynamic modeling and simulation of a variable refrigerant flow air conditioning system," *HVAC&R Research*, vol. 13, no. 2, pp. 243–260, 2007.